 CMES, vol.24, no.3, pp.239-248, 2008

Molecular Dynamics Study of Size Effects and Deformation of Thin Films due to Nanoindentation

Arun K. Nair[1], Diana Farkas[2] and Ronald D. Kriz[1]

Abstract: The indentation response of Ni thin films of thicknesses in the nano scale was studied using molecular dynamics simulations with embedded atom method (EAM) interatomic potentials. Simulations were performed in single crystal films in the [111] orientation with thicknesses of 7nm and 33nm. In the elastic regime, the loading curves observed start deviating from the Hertzian predictions for indentation depths greater than 2.5% of the film thickness. The observed loading curves are therefore dependent on the film thickness. The simulation results also show that the contact stress necessary to emit the first dislocation under the indenter is nearly independent of film thickness. The deformation mechanism consists of the emission of dislocation loops in the area underneath the indenter. The loops are emitted in multiple directions with more dislocations emitted as the films thickness increases. This effect is interpreted as due to the back stress created by the first dislocations emitted when they reach the film/substrate interface and cannot cross into the substrate.

Keyword: Embedded atom method, molecular dynamics, indentation, Nickel, Thin films.

1 Introduction

Nanoindentation is a widely used testing method for the study of material properties of thin films. It is derived from a conventional hardness test and it is routinely used for evaluation of the elastic modulus besides the hardness. In current instruments, the penetration depth can be in the nanometer range, hence the name 'nanoindentation' technique. A common assumption in the modeling and analysis of indentation is that the indented medium is semi-infinite. However, in many nanoindentation tests the analyzed material is a thin film, deposited on a substrate that can itself be a nano-scale film. These problems are of great interest due to the vast applications of thin film structures and the miniaturization of many devices and components. Nanoindentation based technology has thus been developed in the recent years and is an important way of addressing the mechanical properties of thin films, such as hardness. Experimental studies by Gerberich, Nelson, Lilleodden, Anderson and Wyrobek (1996) and Volinsky and Gerberich (2003) have shown that nanoindentation is a reliable and widely used technique for probing mechanical properties of materials.

When addressing properties at the nano-scale new phenomena may appear that are different from the more macroscopic counterparts. For example, the Hall-Petch strengthening with decreasing grain size, typical at the macroscopic scale breaks down at the nanoscale and is actually reversed when the grain sizes are less than 20 nm (Weertman, Farkas, Hemker, Kung, Mayo, Mitra and Van Swygenhoven (1999); Van Swygenhoven, Farkas and Caro (2000); Van Swygenhoven, Caro and Farkas (2001a); Schiotz and Jacobsen (2003); Schiotz (2004)). In another example, size effects have been observed in the mechanical properties of thin FCC films studied by various techniques, including nanoindentation (Espinosa, Prorok and Peng (2004); Espinosa, Panico, Berbenni and Schwarz (2006); Zong, Lou, Adewoye, Elmustafa, Hammad and Soboyejo (2006)).

To completely understand mechanical behavior at the nano scale, molecular dynamics computer

[1] Department of Engineering Science and Mechanics, Virginia Tech, Blacksburg, VA, 24060.
[2] Department of Materials Science and Engineering, Virginia Tech, Blacksburg, VA, 24060.

simulations can be used to model material behavior under various loading conditions. These simulations can reach now the spatial scales typical of nanoindentation and can provide great detail about the mechanisms underlying materials response. Simulations have been used extensively in the past to study the indentation problem and have provided great insight into the actual process of emission of the first dislocations responsible for incipient plasticity as the films are indented (Christopher, Smith and Richter (2001); Li, Van Vliet, Zhu, Yip and Suresh (2002); Lilleodden, Zimmerman, Foiles and Nix (2003); Ma and Yang (2003); Lee, Park, Kim, Jun and Im (2005); Shiari, Miller and Curtin (2005); Iglesias and Leiva (2006); Kim, Yoon, Cho and Jang (2006)). Christopher, Smith and Richter (2001) have shown that atomistic modeling was able to reproduce the experimental features like piling-up of material along the indenter sides. Studies conducted by Li, Van Vliet, Zhu, Yip and Suresh (2002) described the incipient plasticity due to indentation using atomistic simulation and finite element-modeling for Al. Atomistic/continuum modeling of nanoindentaion was also carried out by Shiari, Miller and Curtin (2005) and Iglesias and Leiva (2006). Similar work has been carried out by Ma, Lu, Wang, Roy, Hornung, Wissink and Komanduri (2005) and Ma, Liu, Lu and Komanduri (2006). Lee, Park, Kim, Jun and Im (2005) have also modeled Al and described in detail the homogenous nucleation of dislocations. Szlufarska (2006) and .Schuh (2006) have reviewed recent advances in nanoindentation studies by atomistic modeling. Atomistic simulations also provide trends and information on the mechanisms of plasticity. Most of these studies have been performed in single crystal samples. The effects of random high angle grain boundaries present have been studied by .Hasnaoui, Derlet and Van Swygenhoven (2004). Their work showed that the grain boundaries can emit, absorb and repel dislocations. The effects of thickness and geometry of the indenter in nanoindentation of Ni thin films were studied by Parakala, Mirshams, Nasrazadani and Lian (2004), showing that there is an indentation size effect irrespective of indenter tip geometries.

Nix and Gao (1998) have modeled indentation size effects at the micro scale using the concept of geometrically necessary dislocations and found that hardness increases as depth decreases. However, the model does not address the hardness-depth relation for indentation at the nano-scale. Huang, Zhang, Hwang, Nix, Pharr and Feng (2006) developed an analytical model applicable to indentation at the nanometer scale based on maximum allowable geometrically necessary dislocations. Recently, .Cordill, Chambers, Lund, Hallman, Perrey, Carter, Bapat, Kortshagen and Gerberich (2006) compared the linear and parabolic hardening models in ultra-small cubes and films and found out that linear hardening model gave a better representation of the early trends in experiments; whereas parabolic hardening model fits later stages Zhang, Saha, Huang, Nix, Hwang, Qu and Li (2007) modeled Tungsten films deposited on an Aluminum substrate using conventional mechanism of strain gradient plasticity theory (CMSG), showing that hardness at the microscopic scale decreases monotonically as the indentation depth increases and doesn't reach a constant macroscopic hardness. Indentation size effects studies using plasticity theories are also done by Saha, Xue, Huang and Nix (2001), .Abu Al-Rub and Voyiadjis (2004) and Qu, Huang, Pharr and Hwang (2006). Chen, Liu and Wang (2004) studied the size dependence in Al films on glass and showed that the hardness increases when the tip approaches the film/substrate interface.

In the present work we address the effects of film thickness on indentation response, both in the elastic and the plastic regimes of single crystal films of varying thicknesses and study the deformation mechanism in the plastic regime. We choose for this investigation films of Ni that are oriented in the [111] direction and described by an embedded atom method interatomic potential (EAM) (Daw and Baskes (1984), Finnis (2003)). The elastic responses of the films are compared with Hertzian theory. The technique for the simulation is classical molecular dynamics. The goal of the investigation is to elucidate the effects of film thickness on the elastic and plastic behavior

2 Sample preparation

In order to study the thickness effects due to indentation, samples of single crystal films were generated for different thickness. We generated samples of 7nm and 33nm by changing the dimension of the film along [111] direction (Figure 1). The dimensions of 52nm along the direction and 52nm along the direction were chosen so that the sample is significantly larger than the indentation contact area at maximum depth (10nm) and the spurious effects originating from the finite size of the sample in these directions can be avoided. Before the indentation process, all the samples were relaxed for 100 ps at 300°K using molecular dynamics as implemented in the LAMMPS code (Plimpton (1995)). This relaxation was performed with free surface boundary conditions for the top of the film and a fixed layer of atoms to represent the substrate. The boundary conditions in the directions contained in the film are periodic.

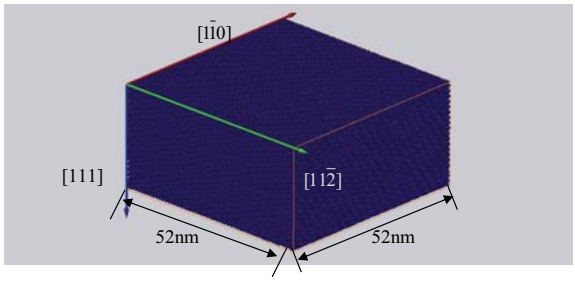

Figure 1: Orientation and size of the single crystal films used in the indentation simulations.

3 Indentation Simulation Procedure

3.1 Interatomic potentials

The embedded atom method is currently a common technique used in molecular dynamics computer simulation of metallic systems (.Daw and Baskes (1984)). The method provides a good description of the interatomic forces in the system, particularly for fcc metals. It calculates the interatomic potentials in metals and models forces between atoms as follows:

$$E = \frac{1}{2}\sum_{i,j} V(r_{ij}) + \sum_i F(\rho_i), \quad \rho_i = \sum_j \varphi(r_{ij}) \quad (1)$$

Where E is the total energy of the system, $V(r_{ij})$ represents the pair interaction energy between an atom i and its neighboring atom j, $\phi(r_{ij})$ is the electronic density function, and $F(\rho_i)$ represents an embedding function accounting for the effects of the free electrons in the metal (Finnis (2003)). In particular, we used the Ni potential functions developed by Voter (1987). These potentials reproduce the perfect lattice properties well and have been tested extensively.

The molecular dynamics algorithm is used here as implemented in the LAMMPS code by Plimpton (1995). The boundary conditions used are periodic in the directions that are perpendicular to the indentation force. The sample sizes in the directions perpendicular to the indentation direction were chosen to be large enough to avoid spurious effects of the periodic boundary conditions used in these directions. In the direction of the indentation force we used a free surface boundary condition for the top of the film and a fixed boundary condition for the bottom of the film, representing a hard substrate. For the indenter, we use a totally rigid spherical indenter with a force on each atom given by Plimpton (1995). The force exerted by the indenter is given by::

$$F(r) = -k(r-R)^2 \quad (2)$$

Where k is the specified force constant equal to10 eV/A^2, r is the distance from the atom to the center of the indenter, and R is the radius of the indenter equal to 15 nm. The force obtained using equation (2) showed excellent agreement with the force computed from pressure in the [111] direction from the LAMMPS output in the elastic regime.

Our samples contain up to 8 million atoms. We typically use 256 processors and each indentation simulation for the larger size takes about a week of computational time.

3.2 Indentation simulation and visualization of the results

The simulations were performed using the LAMMPS code (Plimpton (1995)) in which a rigid spherical indenter with a radius of 15 nm was chosen. The indention process was started by lowering the indenter down the [111] direction into the two thin films at the rate of 1nm per 100 ps. This rate is much faster than in experiments, and is a result of the limitations of the molecular dynamics technique, even using massively parallel simulations, as we do here. The simulation was performed at 300°K with the bottom three atomic layers fixed in the direction. The top of the film surface was treated as a free surface. Periodic boundary conditions were imposed in the- and directions. The atomic positions are monitored at 10 ps intervals until the indentation process is completed after the tip reaches a maximum depth. The force from the indenter is obtained using the atomic positions corresponding to each time step and the force given by equation (2). Contact stresses are obtained as force divided by contact area with the contact area between the indenter and the film is given by:

$$\text{Area} = \pi(2Rd - d^2) \tag{3}$$

Where R is the radius of the indenter and d is the indentation depth.

In order to selectively visualize interior defects, we have employed a visualization technique based on the centrosymmetry parameter that was proven effective for the studies of dislocation emission in FCC crystals and is described by .Kelchner, Plimpton and Hamilton (1998). Centrosymmetry parameter values between 3 and 20 are typical of dislocation cores and stacking faults. Values of the centrosymmetry parameter larger than 20 correspond to atoms at the surface. The atoms with centrosymmetry parameter lower than 3 are located near perfect lattice positions and are not displayed for visualization purposes.

4 Results and Discussion

4.1 Effect of film thickness in the elastic regime

Force versus indenter displacement results in the elastic regime are plotted for the films of two different thickness in Figure 2. The Hertzian theory (Johnson (1985)) prediction for a semi-infinite film indented by a spherical indenter is also shown for comparison. The force in Hertzian theory is given by:

$$P = (4/3)ER^{1/2}h^{3/2} \tag{4}$$

Where E is the modulus of elasticity of Ni (220 Gpa), R radius of the indenter of 15 nm and h is the indentation depth. These results show that indentation into these thin films only follow the Hertzian predictions for a semi-infinite crystal in the very initial stages of the indentation. These results show that in the elastic region, the thinner films require higher forces to achieve the same indentation depth than the thicker films. As expected, the deviation from the Hertzian theory is larger for the thinner films.

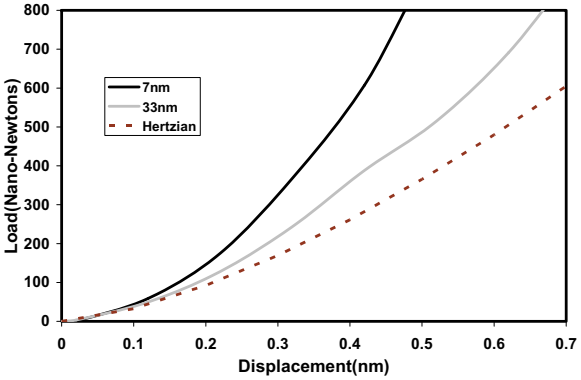

Figure 2: Force versus indenter displacements curves obtained in the elastic regime for films of 7nm and 33nm thicknesses. The Hertzian theory predictions for a semi-infinite film are shown for comparison along 7nm and 33nm films thicknesses.

4.2 Effect of film thickness on the initial plastic event

Figure 3 a shows the forces for which the first dislocation is emitted under the indenter, constituting the initial plastic event. The force values depend on film thicknesses, with the first dislocation appearing at lower indentation depths and requiring higher forces for the thinner films.

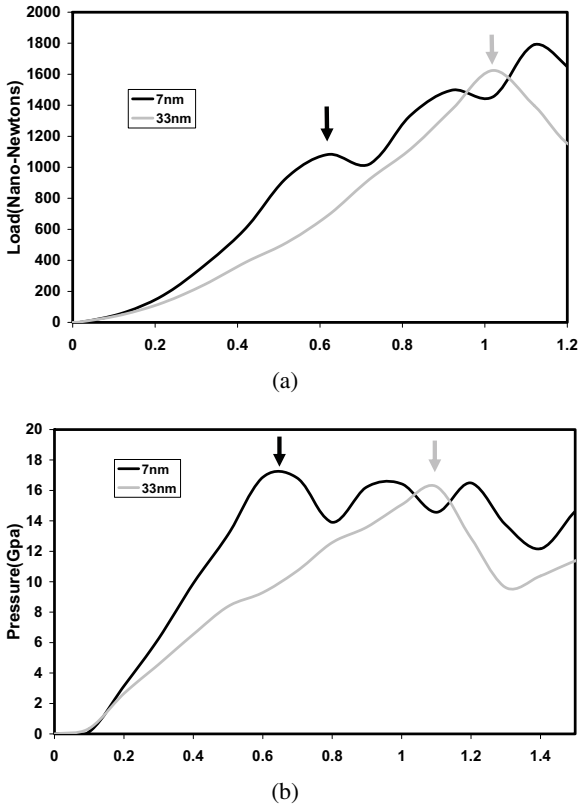

Figure 3: The initial plastic event indicated by the arrows for films of both thicknesses. (a) Force versus indenter displacements curves. (b) Contact pressure (GPa) vs. indenter displacement curves.

In order to find the stress required to emit the first dislocation and to observe the effect of thickness in single crystal films, the contact pressure under the indenter on the film surface was plotted against the indentation depth for different values of film thickness, as shown in Figure 3b. The contact pressure was calculated from the force of the indenter and the contact areas directly observed in the sample. As the film thickness increases, the first dislocation appears at larger indentation depths. However, the contact pressure necessary for the initiation of plasticity in these single crystal films is mostly independent of the film thickness. This implies that the contact stress required for the emission of the first dislocation is not significantly dependent on the film thickness, and independent of the different elastic deformation and stress fields created by the indentation of films of various thicknesses. The contact pressure under the indenter necessary for the homogenous nucleation of the first dislocation is a material dependent quantity and is not affected by film thickness. The thickness independent contact pressure for our [111] single crystal film is approximately 16 GPa. This value is almost half the value (28 Gpa) previously reported by authors Nair, Parker, Gaudreau, Farkas and Kriz (2008) using interatomic potential developed by .Mishin, Farkas, Mehl and Papaconstantopoulos (1999).This clearly indicates that the interatomic potential used for simulations also affects the hardness value Hardnesses of 5 to 6 GPa were experimentally observed in the nanoindentation of Ni films with the (100) orientation Zong, Lou, Adewoye, Elmustafa, Hammad and Soboyejo (2006) at a depth between 0.01μm and 0.1μm. Pan, Nieh and Chen (2006) report experimental values of 6 to 7 GPa for nanocrystalline Ni. One important reason why the value obtained in the simulations is higher is the fact that the experiments are performed on films that contain grain boundaries and other defects, providing sites for heterogeneous nucleation of dislocations.

It is shown in the current study that the critical stress needed to initiate plasticity in single crystals through homogeneous nucleation of dislocations is independent of the film thickness. Several experimental studies (.Uchic, Dimiduk, Florando and Nix (2004); Greer, Oliver and Nix (2005); Volkert and Lilleodden (2006)) have shown that the onset of plasticity in micro and nano pillars is size-dependent. This suggests that in these experiments heterogeneous nucleation of dislocations is responsible for the onset of plasticity. Indeeed Nair, Parker, Gaudreau, Farkas and Kriz (2008) using interatomic potential developed by

Mishin, Farkas, Mehl and Papaconstantopoulos (1999) showed that when defects are present in the films and the dislocations nucleate at these defects, the stress required for this process can be dependent of the thickness.

Another reason why the hardness obtained in the simulations can be higher than the experimental values is that hardness increases with decreasing penetration depth. Zong, Lou, Adewoye, Elmustafa, Hammad and Soboyejo (2006) have reported that this phenomenon is significant in the nanoscale and the hardness increases by a factor of 2 when depth decreases from 500 to 30nm. In addition, Zhang, Saha, Huang, Nix, Hwang, Qu and Li (2007) and Qu, Huang, Pharr and Hwang (2006) found similar effects at the micron to submicron scale.

Hence the value of 16 GPa for the initial plastic event is reasonable for the hardness of Ni thin films at the nanoscale, considering our indentation depths are less than 10 nm.

4.3 The plastic region

Figure 4 shows the full results for the indentation process well into the plastic region. Figure 4a shows the results in terms of the loading curves and figure 4b shows the contact pressure curves. The results indicate that the thinner films are harder in the plastic regime, due to the effects of the substrate. In order to understand the reasons for this behavior, in the following section we analyze the deformation mechanism in detail.

4.4 Deformation Mechanism in Nanoindentation

The atomistic visualization of the indentation simulations showed the mechanisms responsible for the plastic deformation in these films. In the initial phase of plastic behavior, homogenous nucleation of the dislocations are observed directly under the indenter and as the force of the indenter increases dislocation loops are formed (Figure 5). This phenomenon is consistent with the studies done by Li, Van Vliet, Zhu, Yip and Suresh (2002) and Lee, Park, Kim, Jun and Im (2005) where they observed the incipient plasticity is initiated by the homogenously nucleated glide loops.

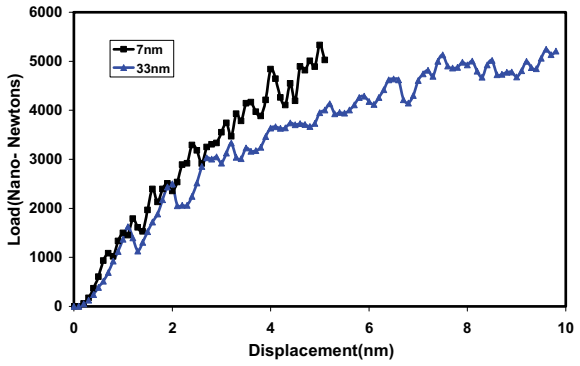

(a)

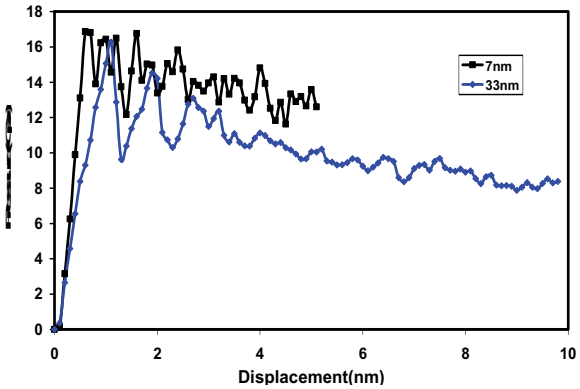

(b)

Figure 4: Loading (a) and Contact pressure (b) vs. indenter displacement curves for films of 7nm and 33nm in the plastic regime.

These dislocation loops then start to grow and expand inside the film and forming prismatic partial glide loops. Figure 5 shows dislocation loops that were observed after the initial dislocation burst for the 33 nm sample at various indentation depths. Figure 6 shows in detail one such prismatic loop, where each side of the loop consists of stacking-fault and are bounded by Shockley partials. The prismatic partial loops glide down to the hard substrate as the indentation depth increases and cannot penetrate the substrate. It gets reflected back as shown in Figure 5. This phenomenon was not observed by Lee, Park, Kim, Jun and Im (2005) for Al since the bottom surface was imposed as a free boundary condition; hence the loop passed through the substrate leaving an impression of a parallelogram. Our simulation also indicates that loops are emitted not only in one direction but in

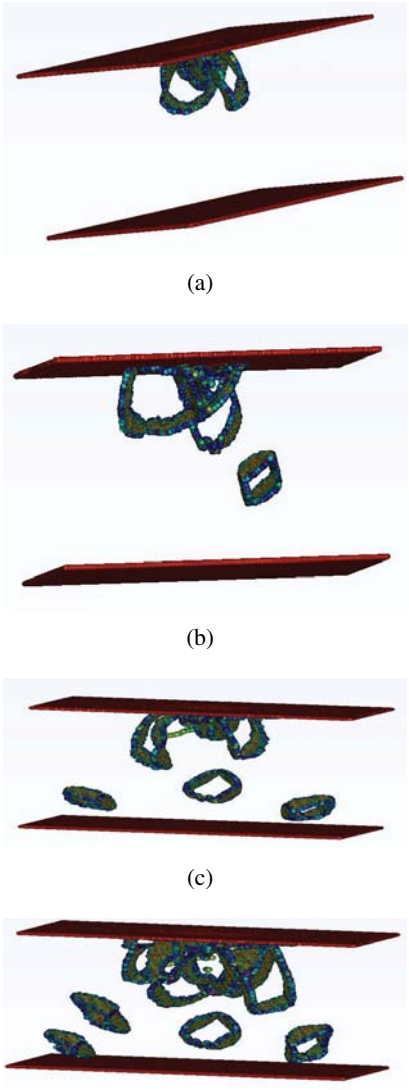

(a)

(b)

(c)

(d)

Figure 5: Visulaization of the dislocation emission process in the 33 nm film due to indentation at depths of (a) 1.2 nm (b) 1.4 nm (c) 1.6 nm (d) 2 nm.

multiple directions (Figure 5 c&d). As the film thickness decreases, loops cannot move as easily due to the fact that there is less space available. In order to understand the effects of this constraint on the plastic deformation process, we analyzed quantitatively the number of dislocations emitted by counting the atoms that have centrosymmetry parameters between 3 and 10 and are located in the dislocations. This number of atoms should be a good quantitative indication of the dislocation

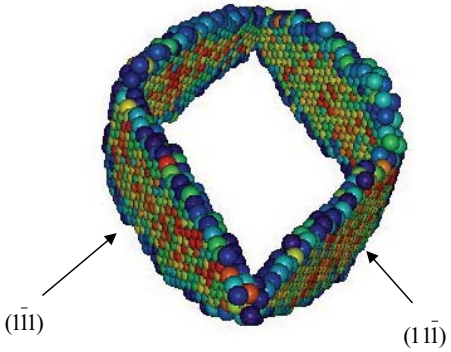

Figure 6: Enhanced view of one of the emitted dislocation loops.

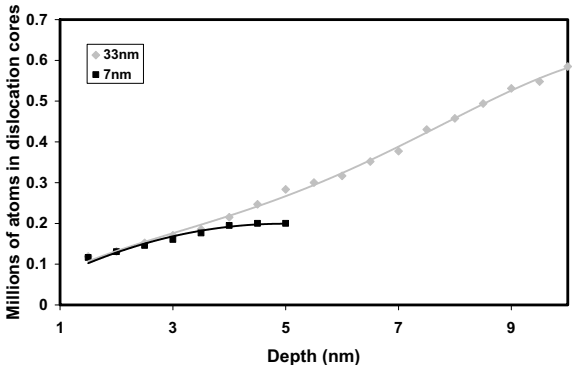

Figure 7: Number of atoms contained in the dislocations emitted for films of 7nm and 33nm versus depth of indentation.

activity as indentation progresses. Figure 7 shows the number of atoms in the dislocations as a function of depth for both films. These results show that film thickness has a significant effect on the number of dislocation emitted. This explains the increased hardness observed for the thinner films.

5 Conclusions

In this paper, we simulated the indentation of Ni [111] thin films of thicknesses 7nm and 33nm using molecular dynamics. The simulations addressed the analysis of thickness, size effect and deformation mechanism of single crystals films and offer a simple explanation for why continuum theories fail to address this issue effectively. Several important conclusions can be drawn from our results.

1. Our results suggest that the contact pressure necessary to emit the first dislocation is a material property in the single crystal films and is mostly independent of film thickness. For Ni described by the potential used here this value is 16 GPa.

2. The deformation mechanism shows, partial prismatic glide loop consisting of stacking-fault bounded by Shockley partials being emitted in multiple directions. These loops get reflected by the hard substrate.

3. The number of dislocations emitted by thin films depends on film thickness, as the films thickness decreases so does the number of dislocations.

References

Abu Al-Rub, R. K.; G. Z. Voyiadjis (2004): Analytical and experimental determination of the material intrinsic length scale of strain gradient plasticity theory from micro- and nano-indentation experiments. *International Journal of Plasticity* **20**(6): 1139-1182.

Chen, S. H.; L. Liu; T. C. Wang (2004): Size dependent nanoindentation of a soft film on a hard substrate. *Acta Materialia* **52**(5): 1089-1095.

Christopher, D.; R. Smith; A. Richter (2001): Atomistic modelling of nanoindentation in iron and silver. *Nanotechnology* **12**(3): 372-383.

Cordill, M. J.; M. D. Chambers; M. S. Lund; D. M. Hallman; C. R. Perrey; C. B. Carter; A. Bapat; U. Kortshagen; W. W. Gerberich (2006): Plasticity responses in ultra-small confined cubes and films. *Acta Materialia* **54**(17): 4515-4523.

Daw, M. S.; M. I. Baskes (1984): Embedded-Atom Method - Derivation and Application to Impurities, Surfaces, and Other Defects in Metals. *Physical Review B* **29**(12): 6443-6453.

Espinosa, H. D.; M. Panico; S. Berbenni; K. W. Schwarz (2006): Discrete dislocation dynamics simulations to interpret plasticity size and surface effects in freestanding FCC thin films. *International Journal of Plasticity* **22**(11): 2091-2117.

Espinosa, H. D.; B. C. Prorok; B. Peng (2004): Plasticity size effects in free-standing submicron polycrystalline FCC films subjected to pure tension. *Journal of the Mechanics and Physics of Solids* **52**(3): 667-689.

Finnis, M. (2003): Interatomic Forces in Condensed Matter. *Oxford University Press*: 129-186.

Gerberich, W. W.; J. C. Nelson; E. T. Lilleodden; P. Anderson; J. T. Wyrobek (1996): Indentation induced dislocation nucleation: The initial yield point. *Acta Materialia* **44**(9): 3585-3598.

Greer, J. R.; W. C. Oliver; W. D. Nix (2005): Size dependence of mechanical properties of gold at the micron scale in the absence of strain gradients. *Acta Materialia* **53**(6): 1821-1830.

Hasnaoui, A.; P. M. Derlet; H. Van Swygenhoven (2004): Interaction between dislocations and grain boundaries under an indenter - a molecular dynamics simulation. *Acta Materialia* **52**(8): 2251-2258.

Huang, Y.; F. Zhang; K. C. Hwang; W. D. Nix; G. M. Pharr; G. Feng (2006): A model of size effects in nano-indentation. *Journal of the Mechanics and Physics of Solids* **54**(8): 1668-1686.

Iglesias, R. A.; E. P. M. Leiva (2006): Two-grain nanoindentation using the quasicontinuum method: Two-dimensional model approach. *Acta Materialia* **54**(10): 2655-2664.

Johnson, K. L. (1985): Contact Mechanics. *Cambridge University Press*.

Kelchner, C. L.; S. J. Plimpton; J. C. Hamilton (1998): Dislocation nucleation and defect structure during surface indentation. *Physical Review B* **58**(17): 11085-11088.

Kim, K. J.; J. H. Yoon; M. H. Cho; H. Jang (2006): Molecular dynamics simulation of dislocation behavior during nanoindentation on a bicrystal with a Sigma=5 (210) grain boundary. *Materials Letters* **60**(28): 3367-3372.

Lee, Y. M.; J. Y. Park; S. Y. Kim; S. Jun; S. Im (2005): Atomistic simulations of incipient plasticity under A1(111) nanoindentation. *Mechanics of Materials* **37**(10): 1035-1048.

Li, J.; K. J. Van Vliet; T. Zhu; S. Yip; S. Suresh (2002): Atomistic mechanisms governing elastic

limit and incipient plasticity in crystals. *Nature* **418**(6895): 307-310.

Lilleodden, E. T.; J. A. Zimmerman; S. M. Foiles; W. D. Nix (2003): Atomistic simulations of elastic deformation and dislocation nucleation during nanoindentation. *Journal of the Mechanics and Physics of Solids* **51**(5): 901-920.

Ma, J.; Y. Liu; H. B. Lu; R. Komanduri (2006): Multiscale simulation of nanoindentation using the generalized interpolation material point (GIMP) method, dislocation dynamics (DD) and molecular dynamics (MD): *CMES: Computer Modeling in Engineering & Sciences* **16**(1): 41-55.

Ma, J.; H. Lu; B. Wang; S. Roy; R. Hornung; A. Wissink; R. Komanduri (2005): Multiscale simulations using generalized interpolation material point (GIMP) method and SAMRAI parallel processing. *CMES: Computer Modeling in Engineering & Sciences* **8**(2): 135-152.

Ma, X. L.; W. Yang (2003): Molecular dynamics simulation on burst and arrest of stacking faults in nanocrystalline Cu under nanoindentation. *Nanotechnology* **14**(11): 1208-1215.

Mishin, Y.; D. Farkas; M. J. Mehl; D. A. Papaconstantopoulos (1999): Interatomic potentials for monoatomic metals from experimental data and ab initio calculations. *Physical Review B* **59**(5): 3393-3407.

Nair, A. K.; Parker, E.; Gaudreau, P.; Farkas, D.; Kriz, R. D. (2008): Size Effects in Indentation Response of Thin Films at the Nanoscale: A Molecular Dynamics Study: to appear in *International Journal of Plasticity*.

Nix, W. D.; H. J. Gao (1998): Indentation size effects in crystalline materials: A law for strain gradient plasticity. *Journal of the Mechanics and Physics of Solids* **46**(3): 411-425.

Pan, D.; T. G. Nieh; M. W. Chen (2006): Strengthening and softening of nanocrystalline nickel during multistep nanoindentation. *Applied Physics Letters* **88**(16):

Parakala, P.; R. A. Mirshams; S. Nasrazadani; K. Lian (2004): Effects of thickness and indenter geometry in nanoindentation of nickel thin films. *Thin Films-Stresses and Mechanical Properties X*. S. G. Corcoran, Y. C. Joo, N. R. Moody and Z. Suo. **795:** 355-360.

Plimpton, S. (1995): Fast Parallel Algorithms for Short-Range Molecular-Dynamics. *Journal of Computational Physics* **117**(1): 1-19.

Qu, S.; Y. Huang; G. M. Pharr; K. C. Hwang (2006): The indentation size effect in the spherical indentation of iridium: A study via the conventional theory of mechanism-based strain gradient plasticity. *International Journal of Plasticity* **22**(7): 1265-1286.

Saha, R.; Z. Y. Xue; Y. Huang; W. D. Nix (2001): Indentation of a soft metal film on a hard substrate: strain gradient hardening effects. *Journal of the Mechanics and Physics of Solids* **49**(9): 1997-2014.

Schiotz, J. (2004): Atomic-scale modeling of plastic deformation of nanocrystalline copper. *Scripta Materialia* **51**(8): 837-841.

Schiotz, J.; K. W. Jacobsen (2003): A maximum in the strength of nanocrystalline copper. *Science* **301**(5638): 1357-1359.

Schuh, C. A. (2006): Nanoindentation studies of materials. *Materials Today* **9**(5): 32-40.

Shiari, B.; R. E. Miller; W. A. Curtin (2005): Coupled atomistic/discrete dislocation simulations of nanoindentation at finite temperature. *Journal of Engineering Materials and Technology-Transactions of the Asme* **127**(4): 358-368.

Szlufarska, I. (2006): Atomistic simulations of nanoindentation. *Materials Today* **9**(5): 42-50.

Uchic, M. D.; D. M. Dimiduk; J. N. Florando; W. D. Nix (2004): Sample dimensions influence strength and crystal plasticity. *Science* **305**(5686): 986-989.

Van Swygenhoven, H.; A. Caro; D. Farkas (2001a): Grain boundary structure and its influence on plastic deformation of polycrystalline FCC metals at the nanoscale: A molecular dynamics study. *Scripta Materialia* **44**(8-9): 1513-1516.

Van Swygenhoven, H.; D. Farkas; A. Caro (2000): Grain-boundary structures in polycrystalline metals at the nanoscale. *Physical Review*

B **62**(2): 831-838.

Volinsky, A. A.; W. W. Gerberich (2003): Nanoindentaion techniques for assessing mechanical reliability at the nanoscale. *Microelectronic Engineering* **69**(2-4): 519-527.

Volkert, C. A.; E. T. Lilleodden (2006): Size effects in the deformation of sub-micron Au columns. *Philosophical Magazine* **86**(33-35): 5567-5579.

Voter, A. F.; Chen, S. P. (1987): High temperature ordered intermetallic alloys. *MRS Symposia Proceedings* **82**: 175.

Weertman, J. R.; D. Farkas; K. Hemker; H. Kung; M. Mayo; R. Mitra; H. Van Swygenhoven (1999): Structure and mechanical behavior of bulk nanocrystalline materials. *Mrs Bulletin* **24**(2): 44-50.

Zhang, F.; R. Saha; Y. Huang; W. D. Nix; K. C. Hwang; S. Qu; M. Li (2007): Indentation of a hard film on a soft substrate: Strain gradient hardening effects. *International Journal of Plasticity* **23**(1): 25-43.

Zong, Z.; J. Lou; O. O. Adewoye; A. A. Elmustafa; F. Hammad; W. O. Soboyejo (2006): Indentation size effects in the nano- and microhardness of fcc single crystal metals. *Materials Science and Engineering a-Structural Materials Properties Microstructure and Processing* **434**(1-2): 178-187.